

Journal of Materials Chemistry A

Accepted Manuscript



This is an *Accepted Manuscript*, which has been through the Royal Society of Chemistry peer review process and has been accepted for publication.

Accepted Manuscripts are published online shortly after acceptance, before technical editing, formatting and proof reading. Using this free service, authors can make their results available to the community, in citable form, before we publish the edited article. We will replace this *Accepted Manuscript* with the edited and formatted *Advance Article* as soon as it is available.

You can find more information about *Accepted Manuscripts* in the [Information for Authors](#).

Please note that technical editing may introduce minor changes to the text and/or graphics, which may alter content. The journal's standard [Terms & Conditions](#) and the [Ethical guidelines](#) still apply. In no event shall the Royal Society of Chemistry be held responsible for any errors or omissions in this *Accepted Manuscript* or any consequences arising from the use of any information it contains.

Solvothermal Synthesis of Hierarchical Eu_2O_3 Nanostructures Templated by Amphiphilic Diblock Copolymer PS-*b*-PMAA: Morphology Control via Simple Variation of Water Content

Ying Xiao^[a], Xiaoyan Wang^[a, b], Thomas Wagner^[c], Jürgen Thiel^[c], Yuan Yao^[d], Yichao Lin^[a], Ezzeldin Metwalli^[d], Rui Liu^[e], Hans Jürgen Butt^[c], Peter Müller-Buschbaum^[d], Jian-Qiang Meng^[b], Liang Chen^[a], Ling-Dong Sun^[e], Chun-Hua Yan^[e], and Ya-Jun Cheng^{*[a]}

[a] Ningbo Institute of Materials Technology and Engineering, Chinese Academy of Sciences, 1219 Zhongguan West Rd, Zhenhai District, Ningbo, Zhejiang Province 315201, P. R. China

E-mail: chengyj@nimte.ac.cn

[b] Tianjin Polytechnic University, State Key Laboratory of Hollow Fiber Membrane Materials & Processes, Tianjin 300387, P. R. China

[c] Max Planck Institute for Polymer Research, Ackermannweg 10, D-55128, Mainz, Germany

[d] Technische Universität München, Physik-Department, Lehrstuhl für Funktionelle Materialien, James-Franck-Str. 1, 85748 Garching, Germany

[e] Beijing National Laboratory for Molecular Sciences, State Key Laboratory of Rare Earth Materials Chemistry and Applications & PKU-HKU Joint Lab on Rare Earth Materials and Bioinorganic Chemistry, College of Chemistry and Molecular Engineering, Peking University, Beijing 100871, P. R. China

Keywords:

Eu₂O₃, Hierarchical Nanostructures, Self-assembly, Solvothermal, Amphiphilic Diblock Copolymer

Abstract

A new method to synthesize hierarchical Eu₂O₃ nanostructures via solvothermal process in N, N'-dimethyl formamide (DMF) templated by an ionic amphiphilic diblock copolymer polystyrene-*block*-poly (methacrylic acid) (PS-*b*-PMAA) has been developed. By simply varying the mass ratio of H₂O over DMF from 0 to 20 wt% in the polymer-salt mixed solution, series of Eu₂O₃ morphologies including worm-like nanoparticles, nanoparticulate mesoporous microspheres, staggered sheets, and sheet-built microspheres are synthesized. The mechanism of the morphology control is the combined effect of both, guiding the Europium salt in the PMAA domains of the micro-phase separated/self-assembled PS-*b*-PMAA, and the hydrolysis-condensation process associated with the solvothermal treatment step.

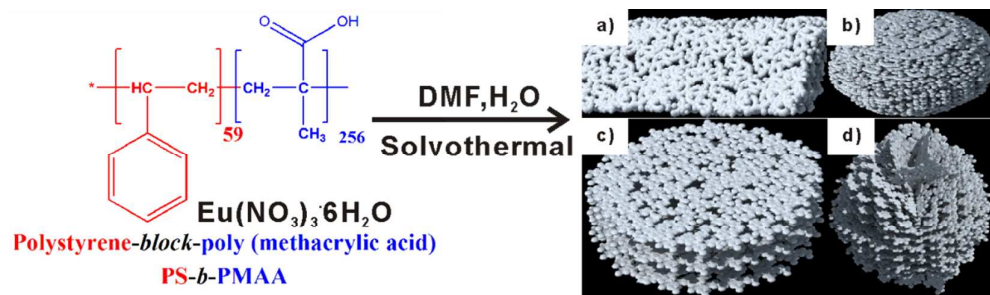
Introduction

Studies on the synthesis of nanostructured rare earth oxides have attracted considerable attention due to their promising applications in up-conversion optics, biomedical devices, catalyst, energy storage, and water treatment¹⁻⁶. Morphology control including shape, size, and assembly of the basic structural units plays an important role for their properties^{1-3, 5-8}. Various strategies have been developed to synthesize nanostructured rare earth oxides with different morphologies such as nanoplates, nanowires, nanodisks, and mesoporous structures^{2, 4, 5, 9-18}. Thermolysis of

rare earth salts in organic solvents has been proved a powerful method to generate a variety of morphologies of different rare earth oxides^{7, 13-15, 19-21}. Non-ionic amphiphilic block copolymers have been also utilized as templating agents to synthesize mesoporous rare earth oxide thin films^{8, 10, 11}. Recently, we proposed to use an ionic amphiphilic diblock copolymer (DBC) polystyrene-*block*-poly (acrylic acid), denoted as PS-*b*-PAA, as a templating agent to synthesize mesoporous rare earth oxide thin films⁹. It is found that PS-*b*-PAA has a universal templating capability to different groups of rare earth oxides from so-called light to medium and to heavy rare earth elements. However, the structures obtained are only in the form of thin films, which significantly limits their potential applications in biomedical devices and catalysis. Hydro/solvothermal reaction has been extensively applied to synthesize metal oxides with various different morphologies in bulk format²². Nevertheless, to the best of our knowledge, the synthesis of bulk nanostructured rare earth oxides templated by amphiphilic block copolymer via hydro/solvothermal reaction has been rarely reported so far.

In the present investigation we report a new strategy to synthesize nanostructured rare earth oxides in bulk format as demonstrated by the synthesis of Eu₂O₃ (**Scheme 1**). An ionic amphiphilic DBC polystyrene-*block*-poly (methacrylic acid) (PS-*b*-PMAA) is used as a templating agent coupled with solvothermal reaction. Effective morphology control is achieved by simply varying the content of water in the DMF solution, where water is a poor solvent for the PS block. Series of different hierarchical structures including worm-like nanoparticles, nanoparticulate

mesoporous microspheres, staggered sheets, and sheet-built microspheres are synthesized.



Scheme 1. Morphology evolution of hierarchical Eu_2O_3 nanostructured powders with increasing water content (from sketch a to d).

The current proposed strategy has two advantages. First, compared to conventional nonionic amphiphilic block copolymer, the PS block and PMAA block have a larger hydrophobicity/hydrophilicity difference, leading to a large Flory–Huggins interaction parameter ($\chi_{\text{PS/PMAA}}$: 0.14 at 160 °C)²³. As a consequence, the formation of stable, large-sized nanostructures via micro-phase separation process is possible. Second, strong interactions between the PMAA block and Eu^{3+} ions can be formed, which significantly enhances the templating effect of copolymer PS-*b*-PMAA. So far, the combination of amphiphilic block copolymer templating process and solvothermal reaction to control the morphology of nanostructured metal oxides has been rarely reported. Thus, insights into the micro-phase separation behavior of amphiphilic block copolymer under solvothermal treatment, and the morphology control of rare earth oxide nanostructures is highly desirable.

Experimental Section

The DBC PS-*b*-PMAA was synthesized via stepwise anionic polymerization

with a PS repeating unit number of 59 and PMAA repeating unit number of 256 (polydispersity index of PS: 1.05, PS volume fraction: 0.25 with the PS density of 1.05 g/cm^3 and PMAA density of 1.275 g/cm^3). Typically, 0.1 g of PS-*b*-PMAA was added to 8.0 g of N, N'-dimethyl formamide (DMF), followed by addition of various amount of water (from 0 g to 1.6 g), and 0.5 g of Europium(III) nitrate hexahydrate ($\text{Eu}(\text{NO}_3)_3 \cdot 6\text{H}_2\text{O}$). Vigorous stirring was applied for 15 min to form a clear solution, which was then transferred into a Teflon-lined solvothermal synthesis reactor of 25 ml capacity. The solvothermal reaction was carried out at $170 \text{ }^\circ\text{C}$ for 12 h in muffle furnace with a ramp rate of 5 K/min starting from room temperature, and cooled to room temperature naturally thereafter. The white precipitates formed were centrifuged and washed several times with DMF. The precipitates were then dispersed in polypropylene glycol (PPG, $M_w = 400 \text{ g/mol}$) to form suspension by ultrasonication for 3 min, followed by addition of diphenyl methane diisocyanate (MDI, 4.13 g) and glycerol (0.4 g). Composite of Eu_2O_3 /polyurethane was formed by gentle heating at 50°C . Finally, the composite was calcined at $800 \text{ }^\circ\text{C}$ in air for 4 h with a ramp rate of 5 K/min to remove the organic materials. The obtained Eu_2O_3 powder was characterized by scanning electron microscopy (SEM), transmission electron microscopy (TEM), small angle X-ray scattering (SAXS), and X-ray photoelectron spectroscopy (XPS), 77.3 K Nitrogen adsorption-desorption, and photoluminescence. Experimental details can be accessed in the supporting information.

Results and Discussions

The morphology change of the hierarchical Eu_2O_3 nanostructures with increasing

mass ratios of H₂O/DMF ($M_{\text{H}_2\text{O}/\text{DMF}}$) templated by PS-*b*-PMAA is shown in **Figure 1** and **Figure S1**. It is found that worm-like Eu₂O₃ nanoparticles with an average length of 108 nm and width of 43 nm are formed without the addition of water. They further aggregate into micrometer sized bulk structures (Figure 1a, Figure S1a, and sketch in Scheme 1). The worm-like nanoparticles represent a typical morphology of metal oxides templated by amphiphilic block copolymers. However, the aggregation of the worm-like nanoparticles into bulk powder is due to the solvothermal treatment. Based on the hard-soft-acid-base (HSAB) theory, strong coordination bond can be formed between “hard” carboxylic acid functional group and “hard” Eu³⁺ ion. Besides, electrostatic interaction between the negative methacrylic acid group and positive Eu³⁺ ion will be established in DMF. The red-shift of the carbonyl stretching band (1648 cm⁻¹ vs. 1716 cm⁻¹) in FTIR proves the complexation of the Eu³⁺ ions with the methacrylic acid functional group (**Figure S2**).

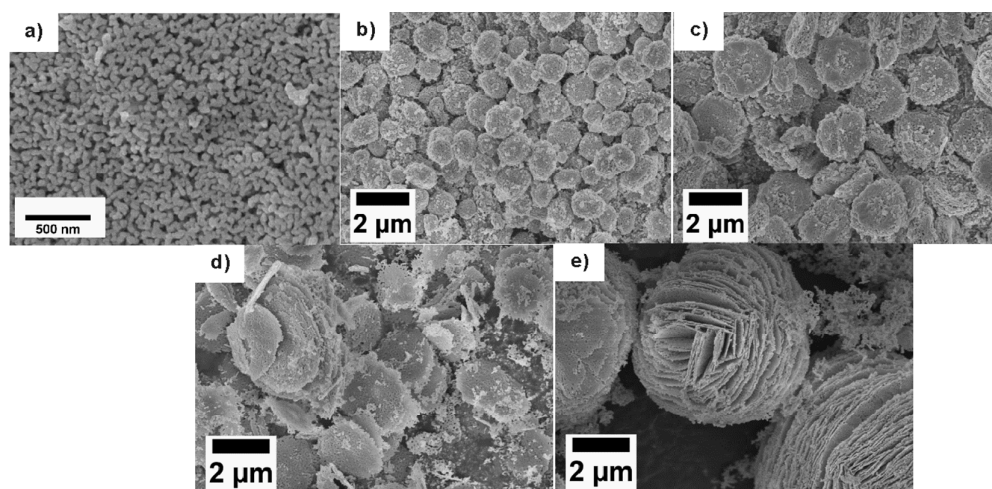


Figure 1. SEM images of the hierarchical Eu₂O₃ nanostructures synthesized with different mass ratios of H₂O/DMF: (a) 0; (b) 2.5 wt%; (c) 5.0 wt%; (d) 10 wt%; (e) 20 wt%. Inset: detailed structure of the sheets assembled into the microspheres.

The hydrolysis-condensation process of the Europium salt is promoted by the solvothermal treatment. It proceeds beyond the domain of single worm-like nanoparticles and consequently individual nanoparticles are connected with each other to form aggregates.

At a water content of 2.5 wt%, the hydrolysis-condensation process is even enhanced by solvothermal treatment due to increased water content. As a result, the worm-like nanoparticles are assembled into mesoporous microspheres with an average diameter around 1 μm (Figure 1b, Figure S1b, and sketch b in scheme 1). When the amount of $M_{\text{H}_2\text{O}/\text{DMF}}$ is further increased to 5.0 wt%, platelet-like structural building blocks are formed instead of worm-like nanoparticles. The platelet structural unit is supposed to originate from the lamellae formed by the microphase separation of PS-*b*-PMAA. The platelets are first assembled together to form two dimensional porous sheets with an average diameter of 2 μm and thickness of 0.8 μm , which are further piled into staggered sheets (Figure 1c, Figure S1c, and sketch c in scheme 1). As water is a poor solvent for the PS block, the increase of water content increases the surface tension between the PS block and solvent. As a result, a morphology transition of the basic structural building block from worm-like nanoparticles into lamella happens. Assisted by the solvothermal treatment, the platelet-like structural building blocks are assembled into sheets and further staggered. When $M_{\text{H}_2\text{O}/\text{DMF}}$ is further increased to 10 wt%, staggered sheets are still observed with the size increased to the range between 2 μm and 5 μm . The increase of the size is attributed to the enhanced hydrolysis-condensation process by increased water content (Figure 1d, Figure S1d).

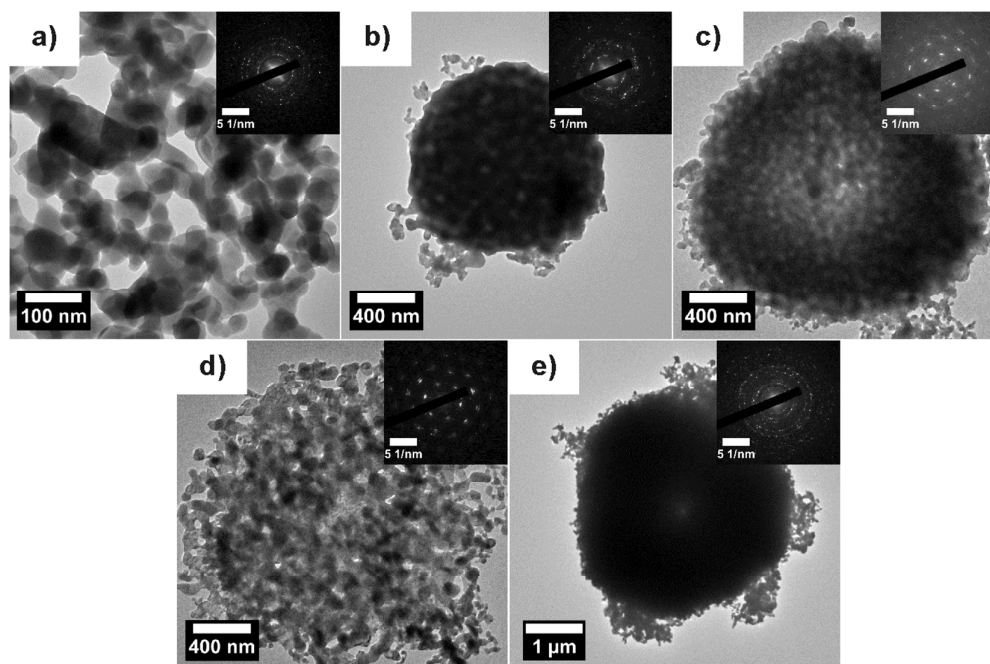


Figure 2. TEM images of the hierarchical Eu_2O_3 nanostructures prepared with different mass ratios of $\text{H}_2\text{O}/\text{DMF}$: (a) 0; (b) 2.5 wt%; (c) 5.0 wt%; (d) 10 wt%; (e) 20 wt%; insets: selected area electron diffraction (SAED) patterns.

At a water content of 20 wt%, sheets are assembled into hierarchical microspheres with an average sphere size of 5 μm - 10 μm (Figure 1e, Figure S1e, and sketch d in scheme 1), which is quite unusual for rare earth metal oxides. The gap between neighboring sheets is in the range between 100 nm and 200 nm. With increasing $M_{\text{H}_2\text{O}/\text{DMF}}$ from 5.0 wt% to 20 wt%, the morphology of the basic structural unit of lamellae templated by PS-*b*-PMAA does not change significantly. However, due to increasing water content, the hydrolysis-condensation process of the Europium salt is enhanced during the solvothermal process. As a result, the assembly process of the lamellae structural building blocks is modified. The average sizes of the sheets and corresponding staggered sheets are enlarged with increasing water content. And finally, spherical assemblies built by the sheets with even larger size are formed.

As a complementary method, transmission electron microscopy (TEM) is applied to further characterize the morphologies of the hierarchical Eu_2O_3 nanostructures (**Figure 2**). Crystalline worm-like nanoparticles are observed in case of $M_{\text{H}_2\text{O}/\text{DMF}} = 0$ (Figure 2a), which is consistent with SEM results. For $M_{\text{H}_2\text{O}/\text{DMF}} = 2.5$ wt%, mesoporous spheres are observed by TEM (Figure 2b), whereas in a range of $M_{\text{H}_2\text{O}/\text{DMF}} = 5.0$ wt% to 10 wt% mesoporous spheres with enlarged size are still presented (Figure 2c and 2d). Because TEM only reflects the shadow of the structures under electron beam illumination, it is difficult to distinguish between true spheres and staggered sheets. However, it is still reasonable that the morphologies observed by TEM agree with the SEM images. With $M_{\text{H}_2\text{O}/\text{DMF}}$ further increased to 20 wt%, thick large spheres with the size of more than $3 \mu\text{m}$ are observed (Figure 2e), which agrees with the three dimensional microspheres observed by SEM. Both, high resolution TEM (HRTEM) (**Figure S3**) and selected area electron diffraction patterns (SAED, inset of each TEM image), prove that the Eu_2O_3 nanostructures are of good crystallinity. This is consistent with the XRD results, which indicate that all of the nanostructured Eu_2O_3 powders obtained after calcination are of cubic phase (PDF No. 65-3182) (**Figure S4**). Thus, the variation of water content only modifies the morphologies of Eu_2O_3 and the crystallographic phase of Eu_2O_3 remains unchanged. The formation of Eu_2O_3 is further proved by X-ray photoelectron spectroscopy (XPS). It confirms the presence of Eu^{3+} within the oxides (**Figure S5**). The peaks at 1164.5 eV and 135.4 eV correspond to the binding energy of the 3d and 4d orbital of Eu^{3+} . The inset of each image shows the details of the 4d electron binding energy spectrum

of Eu ion²⁴.

The measured and simulated small angle X-ray scattering (SAXS) curves are presented in **Figure S6**. The fitting model indicates that the Eu₂O₃ nanoparticulate microspheres prepared with $M_{\text{H}_2\text{O}/\text{DMF}} = 2.5$ wt% possesses very small pores with a diameter of around 3 nm and a size dispersion of 0.50²⁵⁻²⁷. While with increasing amount of $M_{\text{H}_2\text{O}/\text{DMF}}$, the staggered sheets exhibit large porosity with high polydispersity that are featureless in the SAXS data. With $M_{\text{H}_2\text{O}/\text{DMF}}$ increases to 20 wt%, the SAXS profile of the microspheres built by sheets again shows very small pores with a diameter of 1.3 nm and a dispersion of 0.58. The SAXS results are consistent with the SEM and TEM images, where microspheres are built by dense packing of basic structural building blocks.

N₂ adsorption-desorption isotherms are employed to investigate the possible porous structures of the hierarchical Eu₂O₃ nanostructured powders (**Figure S7**). Type IV isotherms with hysteresis loops at high relative pressure are observed with all of the samples. The results imply low porosity and large sized pores with a broad size distribution exist in the powders. The shape of the hysteresis loop belongs to H3, indicating the presence of slit like pores, which is consistent with morphologies observed by SEM and TEM. The specific surface area of the worm-like nanoparticles is 18 m²/g. With the morphology changed to mesoporous microspheres and staggered sheets, the specific surface areas are gradually decreased to 14 m²/g and 11 m²/g. However, regarding the spherical assemblies, the specific surface area is slightly increased to 14 m²/g. The results suggest that the formation of hierarchical spherical

assemblies creates additional pores within the powders and effectively increases the specific surface area.

The templating role of PS-*b*-PMAA on the formation of the Eu₂O₃ nanostructures with different morphologies is proven by investigating samples without using the DBC. Eu₂O₃ powders are prepared following the same protocol without the PS-*b*-PMAA DBC involved. **Figure S8** shows that without the DBC PS-*b*-PMAA, only irregular Eu₂O₃ nanoparticles are formed and randomly aggregated together to form bulk powders. It seems that without the DBC PS-*b*-PMAA, the hydrolysis-condensation process of the Europium salt under solvothermal treatment is poorly controlled. The results imply that the DBC PS-*b*-PMAA plays an important role in the formation of the different nanoscale morphologies when different amounts of water are used.

Furthermore, after solvothermal treatment the morphology of the pure DBC PS-*b*-PMAA is investigated by spin coating the solutions on Si (100) substrate. The AFM height and phase images in **Figure S9** show that lamellae, small nanoparticles, and large nanoparticles are formed on the Si substrate with increasing the amount of M_{H₂O}/DMF from 2.5 wt% to 20 wt%. The exact mass ratio ranges of M_{H₂O}/DMF, where certain morphologies are formed, are not identical with the PS-*b*-PMAA/Eu (NO₃)₃ bulk system. It implies that the introduction of Europium nitrate into the solution modifies the microphase separation/self-assembly behavior of PS-*b*-PMAA. However, the appearance of such typical morphologies confirms that the formation of nanoparticles and lamellae morphologies of Eu₂O₃ is due to the templating effect of

the used DBC.

Based on the results addressed above, it is reasonable to say that the formation of the hierarchical Eu_2O_3 nanostructures is the combined effect of DBC templating agent PS-*b*-PMAA and solvothermal treatment (**Scheme 1**). On the one hand, the increasing water content modifies the micro-phase separation behavior of the DBC, leading to a morphology transition of the basic structural building blocks from worm-like nanoparticles to lamellae. On the other hand, the solvothermal treatment promotes the worm-like nanoparticles and lamellae to self-assemble into hierarchical structures. This self-assembly process is further promoted by the enhanced hydrolysis-condensation of Europium salts due to increased water content. As a result, worm-nanoparticles are converted to nanoparticulate mesoporous microspheres. Lamellae are first assembled into porous sheets, and then piled into staggered sheets and microspheres.

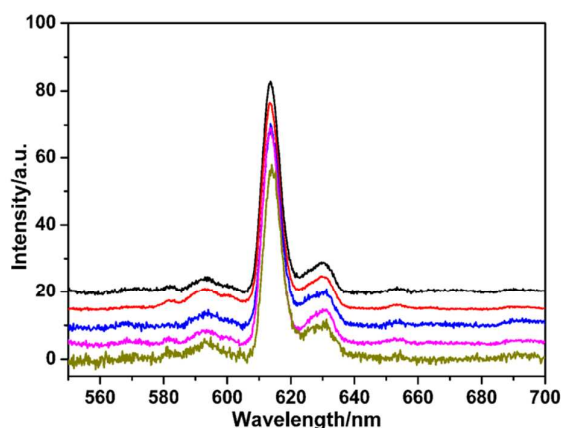


Figure 3. Photoluminescence spectra of the hierarchical Eu_2O_3 nanostructured powders prepared with different mass ratios of $\text{H}_2\text{O}/\text{DMF}$: (black) 0; (red) 2.5 wt%; (blue) 5.0 wt%; (magenta) 10 wt%; (dark yellow) 20 wt%.

Due to its intriguing fluorescence property, Eu_2O_3 has great potential applications for up-conversion material and bioimaging.^{1, 2} Therefore, the photoluminescence properties of the Eu_2O_3 nanostructured powders are investigated. With the excitation wavelength of 254 nm, several peaks appear in the emission spectroscopy (**Figure 3**). The peaks are located at 593 nm ($^5\text{D}_0 \rightarrow ^7\text{F}_1$), 613 nm ($^5\text{D}_0 \rightarrow ^7\text{F}_2$), 630 nm ($^5\text{D}_0 \rightarrow ^7\text{F}_2$), and a weak peak at 650 nm ($^5\text{D}_0 \rightarrow ^7\text{F}_3$). Particularly, it is interesting to note that the integrate intensity ratios of 613 nm over 630 nm vary regarding different Eu_2O_3 nanostructures. With worm-like nanoparticles and nanoparticulate mesoporous microspheres, the ratio value is 3.3. Nevertheless, with the appearance of platelet structure building blocks, the ratio first significantly decreases to 2.4 (nanosheets), then increases to 3.3 (staggered sheets), with a further decrease to 2.4 (microspheres built by packed sheets). It seems that the ratio is related to the morphology of both the basic structural building block (worm-like nanoparticle vs. platelet) and hierarchical structures.

In conclusion, hierarchical Eu_2O_3 nanostructured powders have been successfully synthesized by combing the use of amphiphilic DBC templating agent PS-*b*-PMAA and solvothermal treatment. It is found that the water content plays a vital role in the morphology control of Eu_2O_3 . Basic structural building blocks of worm-like nanoparticles and lamellae of Eu_2O_3 templated by the DBC are formed by increasing water content. Particularly, the worm-like nanoparticles and lamellae structures are self-assembled into mesoporous nanoparticulate microspheres, staggered sheets, and sheet-built microspheres after solvothermal treatment. The

Eu₂O₃ synthesized without the DBC exhibit irregular particles with broad size distribution aggregated into featureless bulk powder. The pure DBC PS-*b*-PMAA also shows lamellae and nanoparticle structures in spin coated films on Si substrates after solvothermal treatment. The photoluminescence property of the Eu₂O₃ nanostructured powders vary with different morphologies.

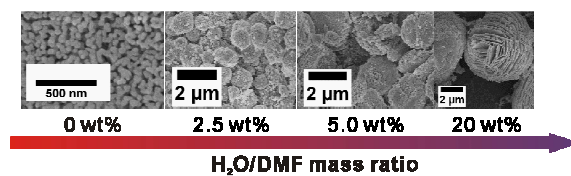
Acknowledgement

This research is funded by the Natural Science Foundation of China (51103172), the Zhejiang Nonprofit Technology Applied Research Program (2013C33190), the Program for Ningbo Innovative Research Team (2009B21008), and Ningbo Key Laboratory of Polymer Materials. Y.Y. acknowledges the China Scholarship Council (CSC) and P.M-B acknowledges the funding by the Nanosystems Initiative Munich (NIM) and the Center for NanoScience (CeNS) Munich.

Supporting Information Available: experimental details of block copolymer synthesis, sample preparation and characterization, SEM, FTIR, HRTEM, XRD, XPS, SAXS, Nitrogen adsorption-desorption isotherm, and AFM of the samples. This material is available free of charge via the Internet at <http://pubs.rsc.org>.

Reference

1. J. Shen, L. D. Sun and C. H. Yan, *Dalton Trans.*, 2008, 5687-5697.
2. G. F. Wang, Q. Peng and Y. D. Li, *Acc. Chem. Res.*, 2011, **44**, 322-332.
3. D. S. Zhang, X. J. Du, L. Y. Shi and R. H. Gao, *Dalton Trans.*, 2012, **41**, 14455-14475.
4. M. Sasidharan, N. Gunawardhana, M. Yoshio and K. Nakashima, *Chem. Lett.*, 2012, **41**, 386-388.
5. M. Sasidharan, N. Gunawardhana, M. Inoue, S. Yusa, M. Yoshio and K. Nakashima, *Chem. Commun.*, 2012, **48**, 3200-3202.
6. J. X. Qu, D. Z. Zheng, X. H. Lu, J. Y. Shi and C. Y. Lan, *Inorg. Chem. Commun.*, 2010, **13**, 1425-1428.
7. R. Si, Y. W. Zhang, L. P. You and C. H. Yan, *Angew. Chem., Int. Ed.*, 2005, **44**, 3256-3260.
8. T. Brezesinski, J. Wang, R. Senter, K. Brezesinski, B. Dunn and S. H. Tolbert, *Acs Nano*, 2010, **4**, 967-977.
9. Y. Xiao, S. S. You, Y. Yao, T. Zheng, C. Lin, S. V. Roth, P. Muller-Buschbaum, W. Steffen, L. D. Sun, C. H. Yan, J. S. Gutmann, M. Z. Yin, J. Fu and Y. J. Cheng, *Eur. J. Inorg. Chem.*, 2013, 1251-1257.
10. C. Reitz, J. Haetge, C. Suchomski and T. Brezesinski, *Chem. Mater.*, 2013, **25**, 4633-4642.
11. J. Haetge, C. Reitz, C. Suchomski and T. Brezesinski, *RSC Adv.*, 2012, **2**, 7053-7056.
12. F. J. Douglas, D. A. MacLaren, C. Renero-Lecuna, R. D. Peacock, R. Valiente and M. Murrie, *Crystengcomm*, 2012, **14**, 7110-7114.
13. D. S. Wang, Z. Y. Wang, P. Zhao, W. Zheng, Q. Peng, L. Q. Liu, X. Y. Chen and Y. D. Li, *Chem. - Asian J.*, 2010, **5**, 925-931.
14. W. Feng, L. D. Sun, Y. W. Zhang and C. H. Yan, *Coord. Chem. Rev.*, 2010, **254**, 1038-1053.
15. Z. G. Yan and C. H. Yan, *J. Mater. Chem.*, 2008, **18**, 5046-5059.
16. T. J. Mullen, M. Zhang, W. Feng, R. J. El-khouri, L. D. Sun, C. H. Yan, T. E. Patten and G. Y. Liu, *Acs Nano*, 2011, **5**, 6539-6545.
17. A. Dorris, C. Sicard, M. C. Chen, A. B. McDonald and C. J. Barrett, *ACS Appl. Mater. Interfaces*, 2011, **3**, 3357-3365.
18. L. E. Englade-Franklin, G. Morrison, S. D. Verberne-Sutton, A. L. Francis, J. Y. Chan and J. C. Garno, *ACS Appl. Mater. Interfaces*, 2014, **6**, 15942-15949.
19. X. Wang, X. M. Sun, D. P. Yu, B. S. Zou and Y. D. Li, *Adv. Mater.*, 2003, **15**, 1442-1445.
20. X. Wang and Y. D. Li, *Angew. Chem., Int. Ed.*, 2003, **42**, 3497-3500.
21. X. Wang and Y. D. Li, *Chem. - Eur. J.*, 2003, **9**, 5627-5635.
22. R. H. Sui and P. Charpentier, *Chem. Rev.*, 2012, **112**, 3057-3082.
23. M. L. Ma, K. Titievsky, E. L. Thomas and G. C. Rutledge, *Nano Lett.*, 2009, **9**, 1678-1683.
24. F. Mercier, C. Alliot, L. Bion, N. Thommat and P. Toulhoat, *J. Electron Spectrosc. Relat. Phenom.*, 2006, **150**, 21-26.
25. E. Metwalli, V. Korstgens, K. Schlage, R. Meier, G. Kaune, A. Buffet, S. Couet, S. V. Roth, R. Rohlsberger and P. Muller-Buschbaum, *Langmuir*, 2013, **29**, 6331-6340.
26. E. Metwalli, I. Krisch, I. Markovits, M. Rawolle, M. A. Ruderer, S. Guo, S. Wyrzgol, A. Jentys, J. Perlich, J. A. Lercher and P. Muller-Buschbaum, *Chemphyschem*, 2014, **15**, 2236-2239.
27. Y. Yao, E. Metwalli, M. A. Niedermeier, M. Opel, C. Lin, J. Ning, J. Perlich, S. V. Roth and P. Muller-Buschbaum, *ACS Appl. Mater. Interfaces*, 2014, **6**, 5244-5254.

Table of Content

Morphology evolution of Eu_2O_3 nanostructures was achieved by simply varying water content, templated by PS-*b*-PMAA under solvothermal treatment.